VOL. 18, NO. 21, NOVEMBER 2023 ISSN 1819-6608
ARPN Journal of Engineering and Applied Sciences

www.arpnjournals.com

WEED DETECTION AND REMOVAL USING ROBOTIC SYSTEM

Puvaneswari G.[1] and Arulselvan S.[2]
[1]Department of Electronics and Communication Engineering, Coimbatore Institute of Technology, Coimbatore, Tamil Nadu, India
[2]Department of Civil Engineering, Coimbatore Institute of Technology, Coimbatore, Tamil Nadu, India
E-Mail: puvaneswari@cit.edu.in

ABSTRACT

Weeding is one of the most significant practices in agricultural production. Weeds are unwanted plants that grow along with the crops and compete with the crops for space, light, water, and soil nutrients. Weeds propagate themselves either through seeding or creeping rootstalk and decrease yields, increase production costs, interfere with the harvest, and lower the product quality. The use of herbicides reduces labor requirements for weed control by up to 60 percent but affects environmental quality and can be toxic to a wide range of organisms. Hence it is necessary to develop an automated system to identify and remove weeds from the vegetable fields. The objective of the proposed work is to develop a mobility level tracked bot that identifies the weeds and removes them with the help of a robotic end effector and to develop a machine learning model to identify the weeds. This functional module will be processed in a Raspberry Pi processor and by using a Raspberry Pi camera module the bot will detect the weeds in vegetable fields. We performed weed detection with different machine learning models like Haar cascade, YOLOv5, and CNN. To evaluate the performance of the machine learning models used, the performance metrics accuracy, precision, recall, and F-measure are estimated and it has been found that CNN has better accuracy, precision, and recall as compared to YOLOv5 and Haar cascade. CNN has the highest F-measure among the three algorithms at 98%. The weed removal is done using a robotic end-effector which is controlled by the Arduino UNO based on the signal from Raspberry Pi.

Keywords: machine learning, weed detection, robot, convolutional neural network, microcontroller.

Manuscript Received 7 September 2023; Revised 7 December 2023; Published 10 January 2024

INTRODUCTION

In the agricultural environment, undesirable plants that are grown along with crops started to create problems as soon as mankind domesticated wild plants (10,000 BC). With the movement of population, unwanted plants spread around the globe and became a problem in some areas. The development of agriculture during Roman times and the middle ages was accompanied by the development of weed removal machinery. From the late 16th century to the early 18th century, weeding was done by workers for low wages. During the late 19th century, with the development of cities, people started to look at alternative methods that reduce the amount of manual weeding by using chemicals.

Weed detection and removal is a task that involves both skill and labor. Nowadays not many people are involved in doing this task. So, farmers are not able to find people who can do this task. This leads to a situation where there is a high need for automating the weeding process. In some existing technologies, weeds are removed using weedicides which will affect the plant's growth and some should be assisted by farmers. Weedicides are the chemicals sprayed on the field to retard the growth of unwanted weeds. But this leads to the phenomenon called bio magnifications. It leads to an increase in the concentration of chemicals at successive tropic levels, which eventually affects the species in the environment.

Two Image driven plant phenotyping methods namely 2-D and 3-D modeling approaches for aiding the selection of crops with early vigor implemented with the selected two triticale genotypes which differ in vigor and growth rate: X-1010 and Triticale1 as model plants by (Shlomi Aharon *et al.*, 2020). The analysis presented shows that both the modeling approaches were sensitive enough to detect the differences in phenotype in just 21 days after sowing and the growth parameters indicated faster early growth of X-1010 genotype. Among the various parameters, the 2-D related parameter Projected Shoot Area (PSA) can be easily extracted via end user-friendly imaging methods, and with PSA, high throughput screening is performed. An Object-based image analysis (OBIA) algorithm on Unmanned Aerial Vehicle (UAV) images by combining Digital Surface Models (DSMs), orthomosaics, and machine learning techniques like Random Forest (RF) to design early post-emergence prescription maps help the farmers in decision-making for optimized crop management. This method also helps to avoid errors due to a subjective manual task. Higher spatial resolution images were used as the ability to discriminate weeds was significantly affected by the resolution and weed density (De Castro, Ana I. *et al.*, 2018). With the help of high spatial resolution (1 cm), UAV-based imagery was used with commercial off the shelf (COTS) digital cameras the calibrated reflectance imagery was controlled and isolation of vegetation canopy reflectance from that of the underlying soil was also performed. To normalize COTS camera imagery for exposure and solar irradiance effects thereby generating multispectral (RGB-NIR) orthomosaics of the target field-based wheat crop trial. The analysis against measurements from a ground spectrometer shows good results for reflectance and Normalized Difference Vegetation Index (NDVI). The impact of canopy cover on NDVI measurements was analyzed and found that in the early

ARPN Journal of Engineering and Applied Sciences

season when canopy development is low, the NDVI values are artificially reduced by the canopy cover (Holman *et al*., 2019). A review of imaging techniques for plant phenotyping assessed a variety of imaging methodologies like visible imaging (machine vision), imaging spectroscopy (multispectral and hyper-spectral remote sensing), thermal infrared imaging, fluorescence imaging, 3D imaging, and tomographic imaging (MRT, PET, and CT) employed for high throughput phenotyping along with their applications (Li *et al.*, 2014).

3D terrestrial remote sensing techniques using Image based point clouds in measuring vegetation biomass and other related structural metrics show that volume and biomass data can be captured using low-cost equipment. Using a 3D point cloud obtained from digital images, surface vegetation biomass in pasture, forest, and woodland environments is analyzed and shows that imaging techniques can be successfully used in vegetation biomass classification (Wallace *et al*., 2017). Machine models like Random Forest (RF), Support Vector Machines (SVM), and K-Nearest Neighbors (KNN) using UAV were found to be efficient in early weed detection and classification (Islam *et al*., 2021 and Kandhasamy *et al*., 2015). A Stereo system to distinguish between the rice crop and weeds in a densely cultivated environment by using machine learning algorithms like artificial neural network (ANN) and two meta-heuristics algorithms like Particle swarm optimization (PSO) and bee algorithm (BA) shows better accuracy in classifying weeds. The proposed approach optimizes the Neural Network for selecting the most effective feature and for the classification of different types of weeds. Firstly, stereo videos are recorded across the rice field; various channels are extracted and decomposed into constituent frames. Secondly, by pre-processing and segmentation of the frames the green plants were obtained from the background. ANN-BA shows better accuracy in weed detection (Dadashzadeh *et al*., 2020 Bakhshipour *et al*., 2018).

Weed detection is also performed using an automated machine vision system. To reduce the excessive use of herbicides in the field, a real time system is used by identifying and spraying the herbicides only on the weeds. Support Vector Machine (SVM) based machine learning models presented 97% accuracy in classifying weeds (Ahmed *et al*., 2012). Least squares discriminant analysis based machine models with better accuracy to detect weeds in wheat fields are proposed by (Herrmann *et al*., 2013). The detection of annual grasses and broadleaf weeds in wheat fields is performed through collection of the ground-level image spectroscopy data, with high spectral and spatial resolutions and the results show that the high resolution images give better accuracy in classifying weeds in wheat fields. Machine learning models using random forest and principal component analysis are used for weed detection with a reduced feature set (Gao *et al*., 2018). With hyper parameter tuning, the accuracy of classification is improved to 95%. Object based image analysis with random forest classifier and maximum likelihood classifier is proposed by (Breiman, 2001). The statistical parameters are used as features for classification and the random forest classifier shows better performance than the maximum likelihood classifier. Commercial unmanned aerial vehicles (UAV) are also used for capturing images in agriculture fields for weed classification. A simple linear iterative algorithm along with a random forest classifier gives better accuracy in identifying weeds in rice fields (Kawamura *et al.*, 2021). Airborne radar data with multi-polarization and textural information is used to differentiate different crops (Anys *et al*., 1995). Histogram based image processing technique is used to identify and differentiate crops. An analysis of labor saving practices in agriculture yield improvement presented by (Asai *et al*., 2017) shows the significance of labor saving practices and their effect on the environment for sustainable development. Hierarchical decomposition based image segmentation was proposed by (Beaulieu *et al.*, 1989) for better accuracy in processing remote sensing data. Picture segmentation is performed using piecewise approximation with minimum error. The interpolated mapping technique is used by (Gerhards *et al*., 1997) in characterizing the spatial stability of weed populations. With the help of this future weed distribution can be predicted but for better prediction, efficient sampling methods are required. The use of IoT in smart farming is analyzed by (Islam et al., 2021 and shows that by integrating different IoT technologies, smart farms can be run with minimum supervision and automated operations.

The existing systems show that image processing and machine learning models can be used in weed detection and removal to improve agriculture production. The efficiency and accuracy of weed detection depend on the performance of machine learning models. Image processing and machine models based robotic systems for weed detection and removal are proposed in this article to overcome the drawbacks of conventional weed detection and removal methods.

The proposed weed detection and removal system will assist the farmers in the weed removal process without affecting the plants and soil nutrition. The existing technologies use different machine learning algorithms that help to identify the weeds and crops in the field. However, the process of removal requires labor. But in this proposed work, a robot is used to remove weeds. The robotic system contains a high resolution camera to capture images of the field. Image processing and machine models are used to identify weeds and a robotic end effector is used to remove the weed from the field.

This proposed work will be a huge benefit to farmers as it reduces their labor to a great extent. The loss encountered by the farmers due to weed is also greatly reduced. This proposed work will be commercially viable and successful as many farmers need this kind of device. The work presented here helps the farmers in automating the process of weed removal without affecting crop growth, thus reducing the time required, and human effort and improving the effectiveness of operation without affecting the soil nutrients and quality. This article comprises the block diagram representation of the weed detection and removal system along with its components,

VOL. 18, NO. 21, NOVEMBER 2023 ISSN 1819-6608
ARPN Journal of Engineering and Applied Sciences

www.arpnjournals.com

machine learning models used, and comparison based on the performance metrics and the hardware and software modules used.

WEED DETECTION AND REMOVAL SYSTEM

This section explains the block diagram of the proposed system and machine learning models used for weed detection. A prototype is developed to implement and test the efficiency of the proposed system.

Proposed System Model

The proposed weed detection and removal system is shown in Figure-1. The working of the entire system is sub divided into three phases: Weed detection by Raspberry Pi, Chassis movement control by Arduino UNO & H-Bridge, and servo arm movement assisted by Arduino UNO. The Raspberry Pi board and the Arduino UNO board are interfaced to enable serial communication between them. The Raspberry Pi Camera module is interfaced with the Raspberry Pi board. The H-Bridge is fed with an input of 12V, which gets distributed among the four DC motors that drive the chassis. The direction of rotation of motors is controlled by the Arduino UNO, through the H-Bridge. All the components are powered by a power bank as a portable power source. At any instant, the camera continuously captures the image and sends it to Raspberry Pi. The captured image is tested against the pre-trained file. If the captured image is identified as cotton, the chassis moves forward and the camera continues to capture the next image. Any plant other than cotton is considered a weed. Hence, if a weed is detected, the Raspberry Pi sends a control signal to the Arduino UNO which operates the Servo Arm, thus removing the weed. After removal, the chassis positions forward and continue the process.

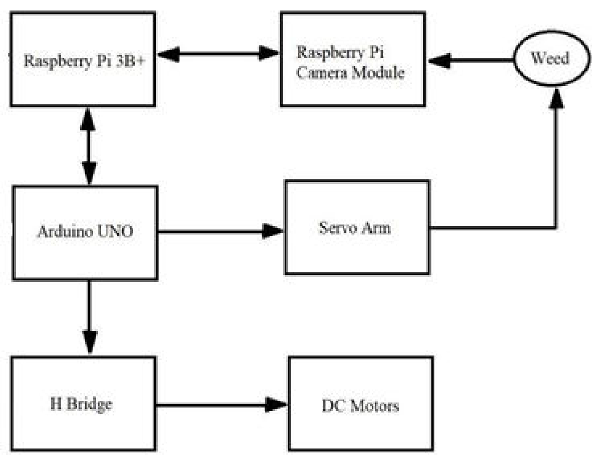

Figure-1. Weed detection and removal system.

Hardware Components

Arduino UNO is a microcontroller board based on the ATmega328P. ATmega328P is the most popular and widely used by beginners and advanced users alike. It is shown in Figure-2.

Figure-2. Arduino UNO.

The board has 14 digital input/output pins out of which 6 can be used as Pulse Width Modulation (PWM) outputs.

It also contains 6 analog inputs, 16 MHz quartz crystal, USB connection, power jack, an ICSP header, and a reset button. Its purpose in this proposed work is to control the movement of chassis, H-Bridge and servo arm. It is an electronic platform used to design and interface different electronic components. It receives signals from many sensors and controls actuators, light etc. Table-1 shows the specifications of the Ardiuno UNO used in developing the system.

Table-1. Specifications of Arduino UNO.

Microcontroller	**ATmega328P-8 bit AVR family microcontroller**
Operating Voltage	5V
Recommended Input Voltage	7-12V
Input Voltage Limits	6-20V
Analog Input Pins	6(A0-A5)
Digital I/O Pins	14
DC Current on I/O Pins	40mA
DC Current on 3.3V Pin	50mA
Flash Memory, SRAM, EEPROM	32KB, 2KB, 1KB
Clock Speed	16MHz

The Raspberry Pi camera module is a small camera that can be connected to a Raspberry Pi computer. It is used to take high-definition video and still photographs. The camera module is capable of 1080p video and still images that connect directly to your Raspberry Pi. It is perfect for time-lapse photography, recording video, motion detection, and security applications. In this project, the camera continuously

VOL. 18, NO. 21, NOVEMBER 2023 ISSN 1819-6608
ARPN Journal of Engineering and Applied Sciences

www.arpnjournals.com

captures the image and sends it to Raspberry Pi. It is shown in Figure-3. Table-2 shows the specifications of it.

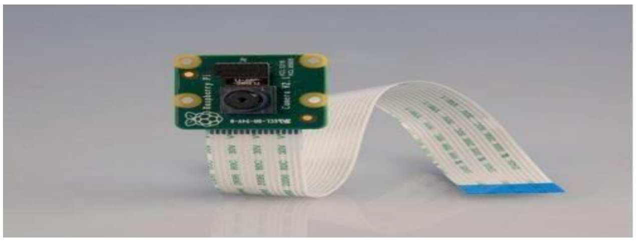

Figure-3. Raspberry Pi camera module.

Table-2. Specifications of camera module.

Image Sensor	**Sony IMX 219 PQ CMOS image sensor**
Resolution	8-megapixel
Still picture resolution	3280 x 2464
Max image transfer rate	1080p: 30fps,720p: 60fps
Connection to RaspberryPi	15-pin ribbon cable
Temperature range	Operating: -20º to 60º C, Stable image: -20º to 60ºC
Dimensions	23.86 x 25 x 9 mm

H-bridge is an electronic circuit that switches the polarity of a voltage applied to a load. These circuits are used in robotics and other application and allow DC motors to run forwards or backwards. It is fed with an input of 12V, which is distributed to the four DC motors. DC motors drive the chassis. Arduino UNO controls the direction of rotation of motors through the H-Bridge. H-Bridge is shown in Figure-4. Table-3 shows the specifications.

Figure-4. H-Bridge.

Table-3. Specifications of H-Bridge.

Double H-Bridge Drive Chip	**L298N**
Logical Voltage	5V
Drive Voltage	5V-35V
Logical Current	0-36mA
Max Power	25W
Dimensions	43 x 43 x 26mm
Weight	26g

The chassis used here is of weight approximately 150g and it is made up of acrylic. It contains 4 motors and its movement is controlled by H-Bridge. Arduino UNO, Raspberry pi, Power bank, H-Bridge and servo arm are mounted on the chassis. The chassis moves across the field where the camera mounted on the chassis captures the images continuously. Figure-5 shows the chassis and Table-4 gives the specification details.

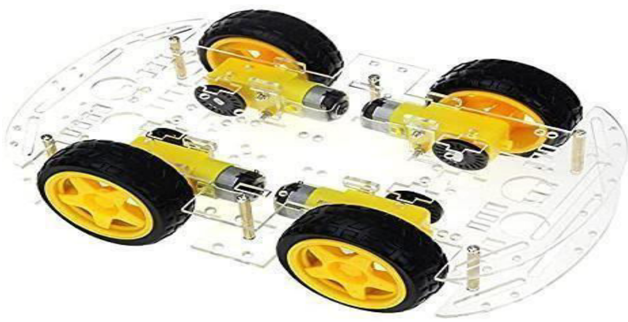

Figure-5. Chassis.

Table-4. Specifications of Chassis.

Operating voltage	**(3 – 12)V DC**
Speed	150 rpm
No load current	40 - 80mA

The Servo arm consists of a pre-assembled robotic gripper and a control switch to open or close the arm. It runs with low rpm and at the base a DC BO geared servo stepper motor is connected. It requires 3-9 V to operate and its movement is controlled by Arduino UNO. When the weed is detected in the field the signal from the Arduino UNO is given to the servo arm and it removes the weed. The servo arm is shown in Figure-6.

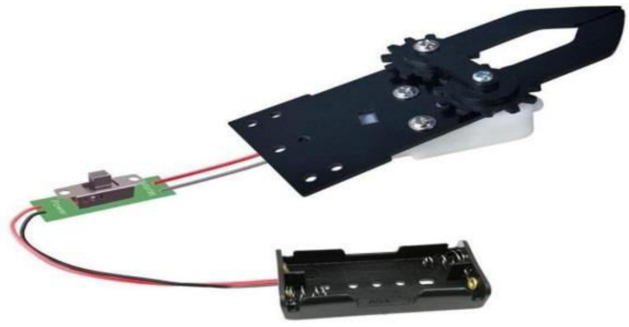

Figure-6. Servo Arm.

A power bank is a portable battery which is used to recharge electronic devices when one do not have access to a regular wall charger. It is essentially a battery inside a metal or plastic enclosure that you can use when there are no outlets available. In this project, all the components are powered by power bank as a portable power source. It is shown in Figure-7 and its specifications are presented in Table-5.

Figure-7. Power Bank.

Table-5. Specifications f Power Bank.

Battery Capacity	**10000 milliamp Hours**
Input	5 V ~ 2.1 A, 9 V ~ 2.1 A, 12 V ~ 1.5A
Output	5 V ~ 2.1 A, 9 V ~ 2.1 A, 12 V ~ 1.5A
Charging power	12 Watts
USB Port	B type port, c type port

The Raspberry Pi 3B+ is a capable little device that enables people of all ages to explore computing and learn how to program in languages like Scratch and Python. Its specifications are presented in table 6 and it is shown in Figure-8.

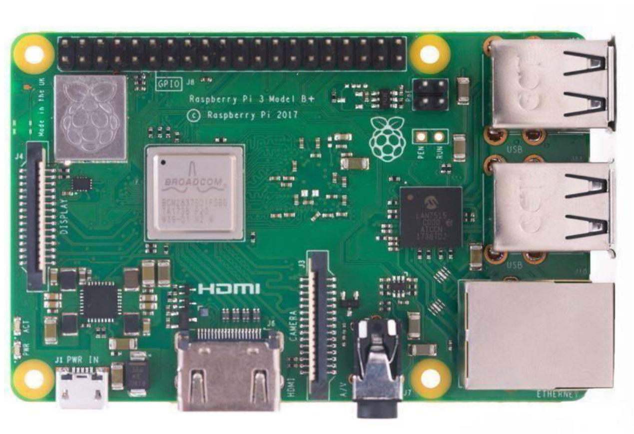

Figure-8. Raspberry Pi 3B+.

Table-6. Specifications of Raspberry Pi 3B+.

SoC	**Broadcom BCM2837B0 quad-core A53 (ARMv8) 64-bit @ 1.4GHz**
GPU	Broadcom Videocore-IV
RAM	1GB LPDDR2 SDRAM
Networking	Gigabit Ethernet (via USB channel), 2.4GHz and 5GHz 802.11b/g/n/acWi-Fi
Bluetooth	Bluetooth 4.2, Bluetooth Low Energy (BLE)
Storage	Micro-SD
GPIO	40-pin GPIO header, populated
Ports	HDMI, 3.5mm analogue audio-videojack, 4x USB 2.0, Ethernet, Camera Serial Interface (CSI), Display Serial Interface (DSI)
Dimensions	82mm x 56mm x 19.5mm, 50g

Haar Cascade Classifier

Haar cascade is an algorithm used to detect objects in an image. For classification, Haar feature based cascade classifiers are used. It contains a lot of positive and negative images to train the classifier model. Each feature in the Haar cascade classifier model is a single value obtained by subtracting the sum of pixels under the white rectangle from the sum of pixels under the black rectangle. The classifier estimates threshold for classification from each feature. To reduce classification error, the features with minimum error rates are used. The Haar cascade classifier is constructed using Haar-like features. These are rectangular patterns of pixel values with alternating light and dark regions. The formula for a Haar-like feature can be expressed as:

$$f(a, b, c, d) = \text{sum}\,(p(a', b') * s(a', b', c, d)) \quad (1)$$

where $(p(a', b')$ is the pixel intensity at location (a', b') in the input image and $s(a', b', c, d)$ is a scaling function that determines the size and shape of the rectangle.
The scaling function is defined as:

$s(a', b', c, d) = 1$, if $a' \leq a + c$ and $b' \leq b + d$ and $a' \geq a$ and $b' \geq b$ (2)

$s(a', b', c, d) = 0$, otherwise (3)

Haar-like features are represented as a vector of rectangular patterns and each pattern is defined by different rectangle sizes and positions. The formula for the Haar cascade classifier is based on a series of decision trees, each of which tests a different Haar-like feature. The output of each decision tree is combined using a weighted sum to produce the final classification result. The formula for the Haar cascade classifier is defined mathematically as:

$$H(x) = \text{sum}(xi * yi(x)) \quad (4)$$

where $H(x)$ is the output of the classifier for the input image x, xi are the weights for each decision tree, and $yi(x)$ is the output of the i-th decision tree.

YOLO

YOLO (You Only Look Once) was proposed in 2015. The YOLO version 5 was introduced in the year 2020. In YOLO, to make final decisions, only one forward pass is required. YOLO consists of three main components: the Backbone, the Neck, and the Head. The Backbone component is the foundation and is used to extract relevant features in an input image. The Neck module is optional in some network architecture and this module is used to refine the features obtained from the Backbone module. This refinement is required to enhance the quality of image representation. The head takes the features from the Neck and performs object detection. The head contains multiple layers to compute bounding boxes and other object related information. All these three components work to achieve better accuracy in object detection. YOLO uses a sum-squared error loss function for optimization and gives balanced weight to the classification problems. There are three terms in the classification loss, the first term calculates the sum-squared error between the predicted confidence score and the second term calculates the mean-squared sum of cells that do not contain any of the bounding boxes. A regularization parameter is used to make this loss small. The third term calculates the sum-squared error of the classes belonging to grid cells.

During object detection, YOLO divides the input image into a grid of S*S size. Each grid predicts the bounding boxes with their confidence score. The confidence score is defined as follows:

$$\text{Confidence score} = \Pr(Object) * Io(truth) \quad (5)$$

The confidence score will be zero when there is no object in the grid. If there is an object present in the image confidence score should be equal to IoU (intersection over union) between ground truth and predicted boxes. The confidence score represents the presence of an object in the bounding box. Each grid in the architecture calculates C conditional class probability, $(Classi|Object)$ which is based on the presence of an object in the grid cell. The number of boxes in each grid cell predicts only one set of the class probabilities. The conditional class probabilities and the individual box confidence predictions are multiplied and confidence scores for each of the boxes are obtained. These scores encode both the probability of that class appearing in the box and how well the predicted box fits an object. It has been observed from the results of the proposed work in weed detection that YOLO performs better than Haar Cascade.

Convolutional Neural Networks

Convolutional Neural Networks (CNNs) are a type of neural network mainlyused for image classification and object detection. Figure-9 shows the CNN architecture. It is formed by stacking three types of layers namely convolutional layers, pooling layers, and fully-connected (FC) layers. In addition to these threelayers, there are two more important parameters which are the dropout layer andthe activation function.

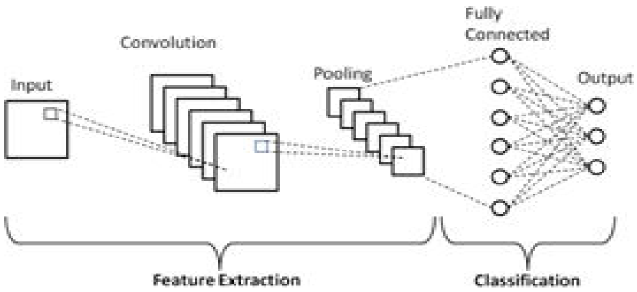

Figure-9. CNN Architecture (Source: Google Images).

The basic CNN is described by a set of formulae for the layers. The first layer of a CNN performs filtering of the input image using convolution operation which is defined by:

$$C[a, b] = \text{sum}(F[m, n] * I[a + m, b + n]) \quad (6)$$

where $C[a, b]$ is the output of the convolution operation at pixel location (a, b), $F[m, n]$ is the filter kernel, and $I[a + m, b + n]$ is the pixel value of the input image at location $(a + m, b + n)$. After convolution, an activation function is applied to the output of each filter. The most common activation function used in CNNs is the Rectified Linear Unit (ReLU) function, which is defined as:

$$f(y) = \max(0, y) \quad (7)$$

where y is the output of the convolution operation. Next pooling operation is performed to reduce the size of the feature maps produced by the convolutional layer. The pooling operations are defined by:

$$P[a, b] = \max(I[(a * stride): (a * stride) + pool(size), (b * stride): (b * stride) + poo(size)]) \quad (8)$$

ARPN Journal of Engineering and Applied Sciences

where P[a, b] is the output of the pooling operation at location (a, b), I is the input feature map, the stride is the stride of the pooling operation and pool($size$) is the size of the pooling window. After the pooling operation, the feature maps are flattened into a vector and passed through one or more fully connected layers. A fully connected layer is mathematically expressed as:

$$Z = f\,(Wx + b) \tag{9}$$

where Z is the output of the fully connected layer, x is the input vector, W is the weight matrix, b is the bias vector, and f is the activation function. The final layer of a CNN is typically a softmax layer, which outputs a probability distribution over the classes. The softmax function:

$$= e^{zi}/\mathrm{sum}(e^{zj}) \tag{10}$$

where P_i is the probability of the i-th class, z_i is the output of the previous layer for the i-th class, e^{zi} is the standard exponential function for the input vector, e^{zj} is the standard exponential function for output vector, and the sum is taken over all classes. It has been observed that CNN comparatively performs better than the Haar Cascade classifier and YOLO.

RESULTS AND DISCUSSIONS

This chapter presents the simulation results of the various machine learning algorithms used for weed detection along with their comparison. It also presents the performance analysis of the Raspberry Pi camera module which is used to capture images of the crops in the field for weed detection and discusses the test results of arm operation in weed removal.

Haar Cascade Classifier

Haar cascade classifier is an object detection algorithm. Initially, the machine learning model for weed detection was developed by using weed images as positive images and cotton images as negative images for training. As training the model for all the types will require more memory and time, another model was developed with the images of the crop as positive images. So, any plant other than the intended plant (cotton here) will be considered a weed by the model, which is an indirect method of weed detection. Figures 10 to 14 present the simulation results for different types of weeds and Figure-15 shows the result obtained for the intended plant.

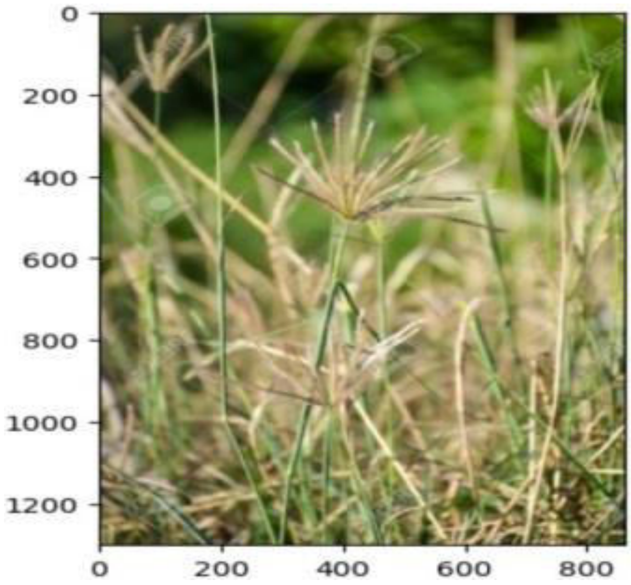

Figure-10. Chloris barbata.

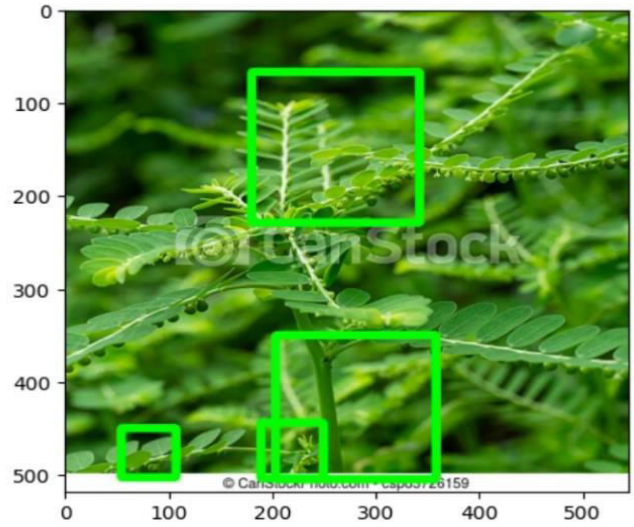

Figure-11. Phyllanthus Niruri.

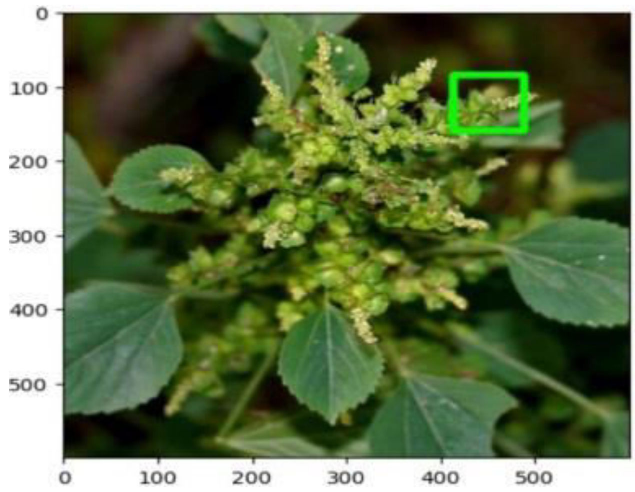

Figure-12. Acalypha Indica.

Figure-13. Trianthema Portulacastrum.

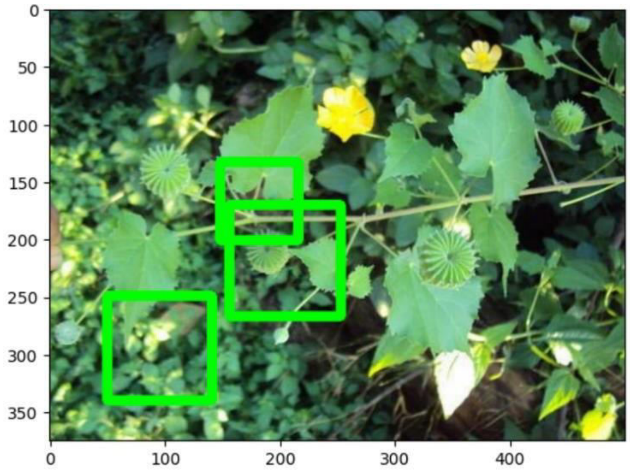

Figure-14. Abutilon Indicum.

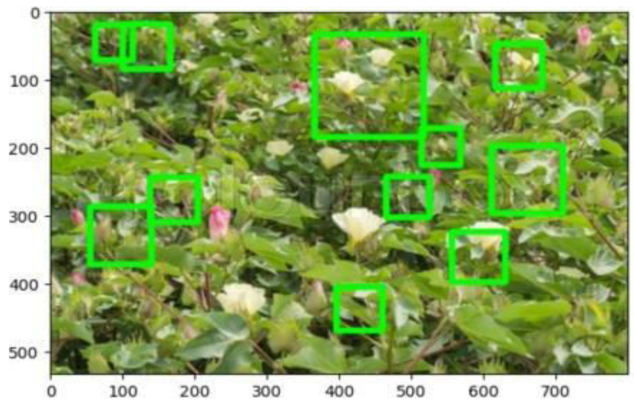

Figure-15. Cotton plant.

In the simulation results, the bounding boxes around the weeds in test images indicate the false positive detections made by the model i.e., the model falsely detects the weeds as cotton. The downside to the Haar cascade is that they tend to be prone to false-positive detections and require parameter tuning when being applied for inference/detection. This greatly reduces the accuracy of the model, thus making it unsuitable for practical implementations. Then the performance of the model was evaluated by forming the confusion matrix and calculating F-measure which was found to be 35%. The percentage of true positives was found to be 20% and that of false positives is 26.67%. Also, the percentage of true negatives was found to be 6.67% and that of false negatives is 46.67%. The performance metrics like F-measure, precision rrecall, and accuracy were calculated and it is shown in Figure-16. It shows the accuracy of classification is 22%.

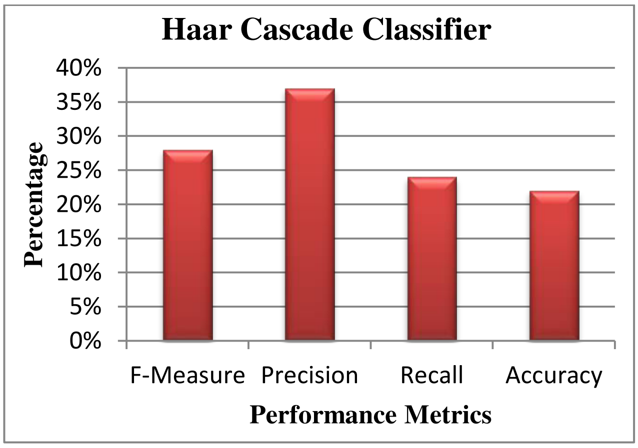

Figure-16. Performance analysis of Haar cascade.

YOLOv5

You Only Look Once (YOLO) is a popular object detection model known for its speed and accuracy. It proposes using an end-to-end neural network that makes predictions of bounding boxes and class probabilities all at once. In the proposed work, YOLOv5 algorithm is used to train the machine learning model. Figures 17 & 18 show the results obtained with YOLOv5 with detections made by the YOLOv5 model upon training for 100 epochs. The confidence of the model over the detection is also displayed along with a bounding box formed around the detected weed as well as an intended plant (cotton).

Figure-17. Weed detection.

VOL. 18, NO. 21, NOVEMBER 2023 ISSN 1819-6608
ARPN Journal of Engineering and Applied Sciences

www.arpnjournals.com

Figure-18. Cotton plant detection.

It can be observed that the confidence score over detection of cotton is 42% for weed images and 70% for cotton plants. A lower score indicates that it is not the intended plant.

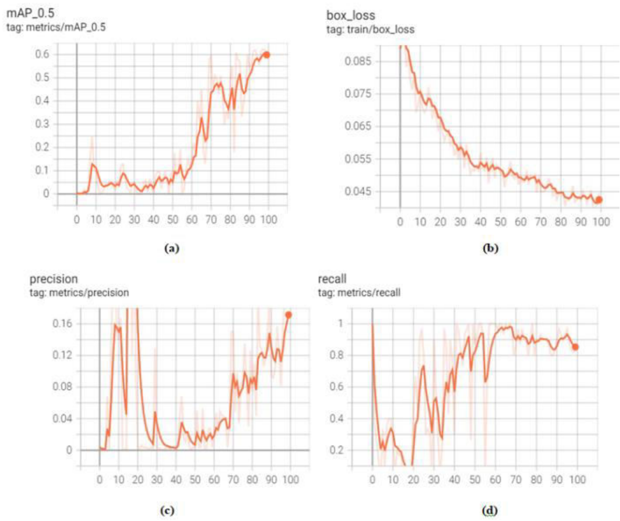

Figure-19. Performance analysis of YOLOv5.

Figure-19 shows the graphs plotted for the various performance parameters. The performance of the model was evaluated by analyzing the training loss, mAP, precision, and recalls parameters against the number of epochs of training given to the model. As the loss decreases, the precision and recall of the model increase with the number of epochs given for training. The percentage of true positives was found to be 15.38% and that of false negatives is 23.01%. Also, the percentage of true negatives was found to be 46.2% and that of false positives is 15.38%. The number of false positive and false negative detections has decreased in YOLOv5 model. The model performance was evaluated using the performance metrics F-measure, Precision, Recall and Accuracy. It can be observed from the measures of performance metrics, YOLOv5 performs better than Haar Cascade Classifier.

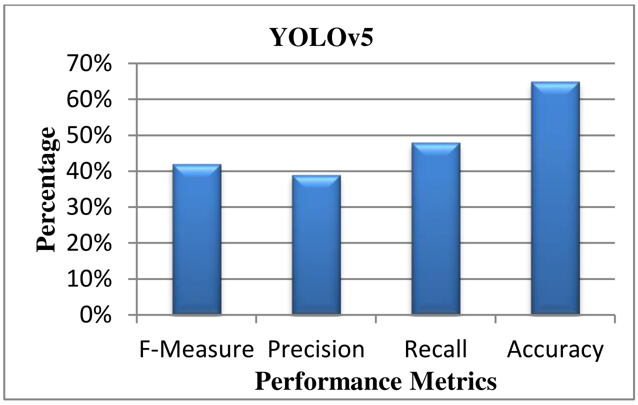

Figure-20. Performance metrics of YOLOv5.

Convolutional Neural Network

Figures 21 and 22 show the results obtained using a convolutional neural network. The percentage of true positives was found to be 42% and that of false positives is 11%. Also, the percentage of true negatives was found to be 39.12% and that of false negatives is 8.3%. The number of correct detections is higher in the CNN model when compared with the previous models.

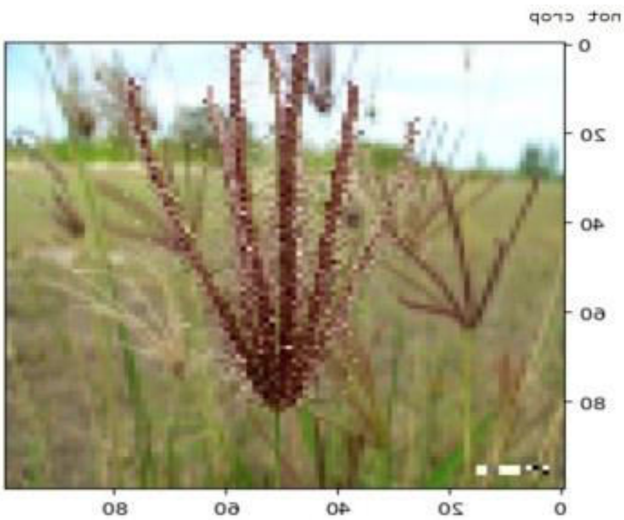

Figure-21. Weed detection.

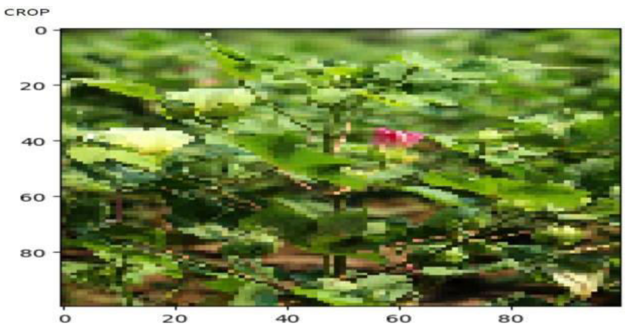

Figure-22. Cotton plant.

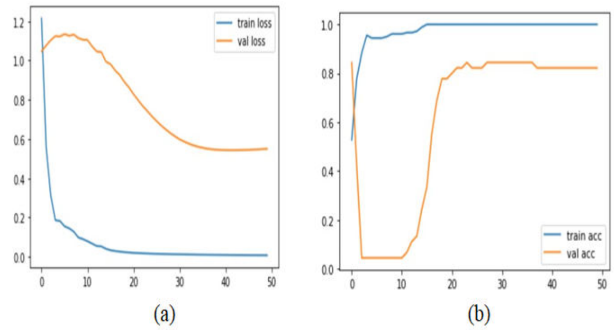

Figure-23. Performance analysis of CNN.

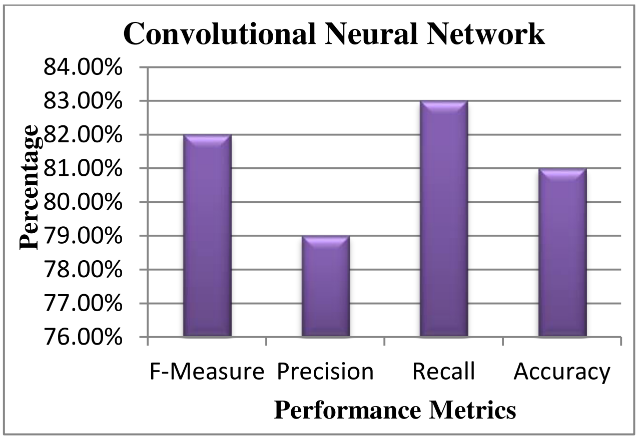

Figure-24. Performance Metrics of CNN.

Figure-23 (a) shows the model's train loss and validation loss plotted against the number of epochs given for training. The training loss decreased rapidly within a few epochs, while the validation loss gradually decreases with the increase in the epochs. Figure-23 (b) shows the training and validation accuracy of the model plotted against the number of epochs given for training. From the plot, wesee that the training accuracy increases rapidly and reaches the maximum value within a few epochs, while the validation accuracy initially decreases with the increase in the epochs, and later around 15 epochs, the accuracy suddenly increased and reached a constant value. Figure 24 shows the performance metrics values obtained for CNN model. It is observed that CNN performs better than other two approaches.

Comparison of Machine Learning Models

Table-7 shows the comparison of the machine models Haar cascade, YOLOv5, and CNN. It can be observed that the convolutional Neural Network model performs better than the other two models. Hence CNN is used in developing the prototype of the proposed weed detection and removal robot.

Table-7. Machine learning model comparison.

Parameters	Harr Cascade Classifier (%)	YOLOv5 (%)	CNN (%)
Accuracy	22	65	81
Precision	37	39	79
Recall	24	48	83
F-Measure	28	42	82

Robotic End-Effector Operation

The CNN algorithm-based machine learning model was developed for weed detection and was integrated with the robotic arm for weed removal. The completed model is shown in Figure-25. The model was then tested in real time to evaluate its performance and to rectify the errors. As any plant other than cotton is considered a weed, the end model was tested using normal plants found in the garden as shown in Figure-26. The real time test result is shown in Figure-28.

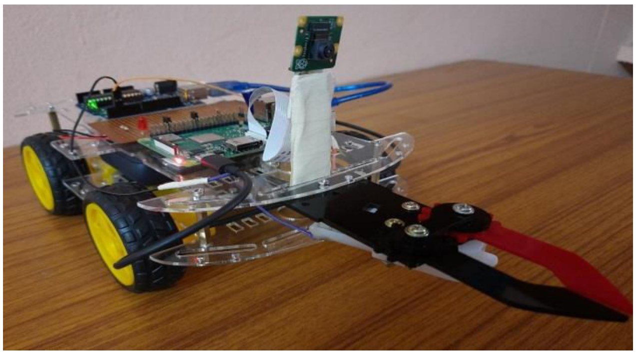

Figure-25. Complete Model.

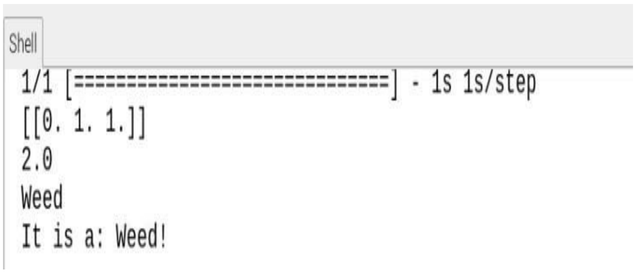

Figure-26. Test result in Thonny IDE.

When the program for weed detection is executed in Thonny IDE, the Raspberry Pi camera module is invoked to capture images. The captured images are stored in a particular location mentioned in the program. The image is then given as input to the machine-learning model for the classification of weeds and plants. Figure-26 shows the result obtained in Thonny IDE. Figure-27 shows the robotic arm operation upon detection of weed by the CNN model. The given input image is classified by the CNN model as weed or crop. If the given image is detected as weed, the Raspberry Pi sends a signal to Arduino to initiate the arm movement for weed removal.

In Figure-27, the arm moves to pluck the weed as the plant is a weed.

Figure-27. Robotic arm operation.

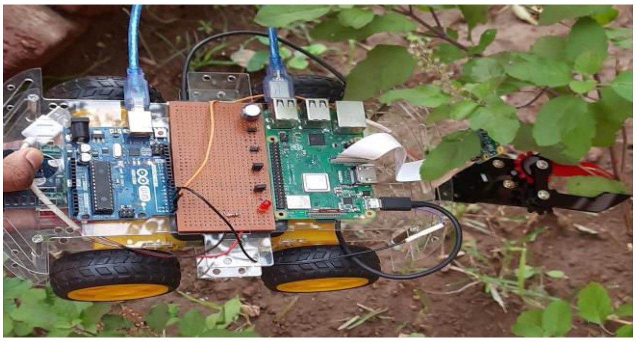

Figure-28. Real time testing.

CONCLUSIONS

The proposed system for weed detection and removal contains a model for automatic detection and removal of weeds using robotic end-effector. The performance of various machine learning algorithms like Haar-Cascade, YOLOv5 and CNN for discriminating crops and weed was analyzed. The robotic end-effector is controlled by the Arduino UNO based on the input signal received from Raspberry pi as a result of image processing. The scope of this proposed work is the detection and removal of weeds for single crop which can be enhanced by implementing the same for multiple crops.

REFERENCES

Shlomi Aharon, Zvi Peleg, Eli Argaman, Roi Ben-David, and Ran N. Lati. 2020. Image-Based High-Throughput Phenotyping of Cereals Early Vigor and Weed-Competitiveness Traits. Remote Sensing. 12(23): 3877-3894.

De Castro Ana I., Jorge Torres-Sánchez, Jose M. Peña, Francisco M. Jiménez-Brenes, Ovidiu Csillik and Francisca López-Granados. 2018. An automatic random forest-OBIA algorithm for early weed mapping between and within crop rows using UAV imagery. Remote Sensing. 10(2): 285-306.

Holman Fenner H., Andrew B. Riche, March Castle, Martin J. Wooster, and Malcolm J. Hawkesford. 2019. Radiometric calibration of commercial off the cameras for UAV-based high-resolution temporal crop phenotyping of reflectance and NDVI. Remote Sensing. 11(14): 1657-1677.

Li Lei, Qin Zhang and Danfeng Huang. 2014. A review of imaging techniques for plant phenotyping. Sensors. 14(11): 20078-20111.

Wallace Luke, Samuel Hillman, Karin Reinke, and Bryan Hally. 2017. Non- destructive estimation of above-ground surface and near-surface biomass using 3D terrestrial remote sensing techniques. Methods in Ecology and Evolution. 8(11): 1607-1616.

Islam Nahina, Md Mamunur Rashid, Santoso Wibowo, Cheng-Yuan Xu, Ahsan Morshed, Saleh A. Wasimi, Steven Moore and Sk Mostafizur Rahman. 2021. Early Weed Detection Using Image Processing and Machine Learning Techniques in an Australian Chilli Farm. Agriculture. 11(5): 387-400.

Dadashzadeh Mojtaba, Yousef Abbaspour-Gilandeh, Tarahom Mesri- Gundoshmian, Sajad Sabzi, José Luis Hernández-Hernández, Mario Hernández-Hernández and Juan Ignacio Arribas. 2020. Weed Classification For Site-Specific Weed Management Using An Automated Stereo Computer-Vision Machine-Learning System In Rice Fields. Plants. 9(5): 559-578.

Kandhasamy J. Pradeep and S. J. P. C. S. Balamurali. 2015. Performance analysis of classifier models to predict diabetes mellitus. Procedia Computer Science. 47: 45-51.

Bakhshipour Adel and Abdolabbas Jafari. 2018. Evaluation of support vector machine and artificial neural networks invweed detection using shape features. Computers and Electronics in Agriculture. 145: 153-160.

Ahmed Faisal, Hawlader Abdullah Al-Mamun, ASM Hossain Bari, Emam Hossain and Paul Kwan. 2012. Classification of crops and weeds from digital images: A support vector machine approach. Crop Protection. 40: 98-104.

Herrmann I., U. Shapira S. Kinast A. Karnieli and D. J. Bonfil. 2013. Ground- level hyperspectral imagery for detecting weeds in wheat fields. Precision Agriculture. 14: 637-659.

Gao, Junfeng, David Nuyttens, Peter Lootens, Yong He, and Jan G. Pieters. 2018. Recognising weeds in a maize crop using a random forest machine- learning algorithm and near-infrared snapshot mosaic hyperspectral imagery. Bio systems engineering. 170: 39-50.

Breiman Leo. 2001. Random Forests. Machine learning. 45: 5-32.

Kawamura Kensuke, Hidetoshi Asai, Taisuke Yasuda, Pheunphit Soisouvanh, and Sengthong Phongchanmixay.

2021. Discriminating Crops/Weeds in an Upland Rice Field from UAV Images with the SLIC- RF Algorithm. Plant Production Science. 24(2): 198-215.

Anys Hassan and Dong-Chen He. 1995. Evaluation of textural and multipolarization radar features for crop classification. IEEE Transactions on geoscience and remote sensing. 33(5): 1170-1181.

Asai Hidetoshi, Pheunphit soisouvanh, Pheng sengxua, Kenichiro Kimura, Banthasack vongphuthine and Masuo ando. 2017. Labor-saving practices for the external expansion of swidden agriculture for upland rice production in a mountainous area of Laos. Tropical Agriculture and Development. 61(4): 166-178.

Beaulieu J-M. and Morris Goldberg. 1989. Hierarchy in picture segmentation: A stepwise optimization approach. IEEE Transactions on Pattern Analysis and Machine Intelligence. 11(2): 150-163.

Gerhards Roland, Dawn Y. Wyse-Pester, David Mortensen and Gregg A. Johnson. 1997. Characterizing spatial stability of weed populations using interpolated maps. Weed Science. 45(1): 108-119.

Islam Nahina, Md Mamunur Rashid, Faezeh Pasandideh, Biplob Ray, Steven Moore and Rajan Kadel. 2021. A Review of Applications and Communication Technologies for Internet of Things (IoT) and Unmanned Aerial Vehicle (UAV) Based Sustainable Smart Farming. Sustainability. 13(4): 1821-1841.